

# Covariance Analysis for On-the-fly ASF Calibration During Multichain Navigation

Jaime Y. Cruz  
Illgen Simulation Technologies, Inc.  
jcruz@illgen.com

## ABSTRACT

This paper describes an all-in-view weighted least squares estimation of a Loran receiver's horizontal position and time bias, with simultaneous (on-the-fly) estimation of additional secondary factor (ASF) errors along the receiver-to-transmitter paths. In this context, the ASF error parameter along a receiver-to-Secondary path absorbs both ASF errors along the receiver-to-Secondary path as well as emission delay (ED) modeling errors arising from ASF errors along the SAM-to-Secondary and SAM-to-Master paths. The estimation is based on time-of-arrival (TOA) measurements and their error covariances, a priori ASFs and their error covariances, and potentially a priori position and time updates from an external source and their error covariances.

For utilizing ASF error calibrations along given paths, an extended form of the usual least squares technique, called least squares collocation, is described for predicting ASF errors at the receiver location based on calibrated ASF errors along arbitrary paths. The calibrated ASFs may come from a previous solution with external position/time update, or in the future may come from a set of ASFs broadcast from a regularly updated calibration.

The required a priori ASF error covariance model is expressed as double path integrals of a postulated homogeneous (location independent) and isotropic (azimuth independent) covariance function describing the spatial distribution of phase velocity errors in the operating area. The assumed phase velocity error covariance function is a function of the distance separation between the points being correlated and parameterized by the variance, which is the value at zero separation, and the correlation length, which is the separation at which the covariance drops to half the variance.

## 1. Introduction

Illgen Simulation Technologies, Inc. (ISTI) is developing an all-in-view Loran-C position algorithm suitable for use in a weighted combined Global Positioning System (GPS)/Loran-C navigation system. The goal of the program sponsoring this work is to show that the Loran-C component of a hybrid system can meet the requirements for horizontal navigation and approach procedures during loss of the GPS signal. This paper focuses on a part of the algorithm system described in [1], namely, the modeling of a priori ASF/ED errors and their treatment in the navigation estimation.

The paper is organized as follows. Section 2 presents the least squares equations used in the covariance analysis of an all-in-view Loran-C navigation with simultaneous (i.e., on-the-fly or OTF) calibration of ASF/ED errors. Section 3 proposes a covariance model for phase velocity errors. Section 4 describes the ASF/ED error covariance model implied by the postulated phase

velocity error covariance model. Section 5 introduces least squares collocation for predicting ASF/ED errors at the user location based on calibrated ASF/ED errors along arbitrary paths. Section 6 gives the covariance equations for analyzing navigation errors implied by various treatments of ASF/ED errors in the estimation. Section 7 gives the verification and validation tests performed on the OTF ASF calibration technique. Finally, Section 8 gives the summary and recommendations.

## 2. Least Squares Estimation Equations

Start with the following non-linear observation model with two groups of parameters and three groups of observations at an epoch:

$$(2-1) \quad \begin{bmatrix} L_{1a} \\ L_{0a} \\ L_{2a} \end{bmatrix} = \begin{bmatrix} F(X_{Aa}, X_{Ba}) \\ X_{Aa} \\ X_{Ba} \end{bmatrix}$$

where:

$F$  ... Known vector function  
 $X_{Aa}$  ... True vector of group-A parameters, containing the user's East, North, and Clock Bias parameters  
 $X_{Ba}$  ... True vector of group-B parameters, containing the additional secondary factors (ASFs) along the receiver-to-transmitter paths  
 $L_{1a}$  ... True vector of group-1 observations, containing the Loran Time-of-arrival (TOA) observations  
 $L_{0a}$  ... True vector of group-0 observations, containing assumed direct observations of the parameters  $X_{Aa}$   
 $L_{2a}$  ... True vector of group-2 observations, containing assumed direct observations of the parameters  $X_{Ba}$ .

The linearized observation equation system becomes:

$$(2-2) \quad \begin{bmatrix} L_{1b} \\ L_{0b} \\ L_{2b} \end{bmatrix} + \begin{bmatrix} V_{1a} \\ V_{0a} \\ V_{2a} \end{bmatrix} = \begin{bmatrix} F(X_{A0}, X_{B0}) \\ X_{A0} \\ X_{B0} \end{bmatrix} + \begin{bmatrix} A & B \\ I & 0 \\ 0 & I \end{bmatrix} \begin{bmatrix} X_{Aa} - X_{A0} \\ X_{Ba} - X_{B0} \end{bmatrix}$$

where:

$\begin{bmatrix} L_{1b} \\ L_{0b} \\ L_{2b} \end{bmatrix}$  ... Observation vector  
 $\begin{bmatrix} V_{1a} \\ V_{0a} \\ V_{2a} \end{bmatrix}$  ... Theoretical residual vector  
 $\begin{bmatrix} X_{A0} \\ X_{B0} \end{bmatrix}$  ... Linearization "point"  
 $\begin{bmatrix} A & B \\ I & 0 \\ 0 & I \end{bmatrix}$  ... Observation partials  
 $I$  ... Identity matrix.

The observation partials are defined as:

$$(2-3) \quad A \equiv \left. \frac{\partial F}{\partial X_{Aa}} \right|_{X_{Aa}=X_{A0}} ; \quad B \equiv \left. \frac{\partial F}{\partial X_{Ba}} \right|_{X_{Ba}=X_{B0}}$$

The linearized observation equation system can be written as:

$$(2-4) \quad \begin{bmatrix} V_{1a} \\ V_{0a} \\ V_{2a} \end{bmatrix} = \begin{bmatrix} A & B \\ I & 0 \\ 0 & I \end{bmatrix} \begin{bmatrix} X_A \\ X_B \end{bmatrix} - \begin{bmatrix} L_1 \\ L_0 \\ L_2 \end{bmatrix}$$

with the following definitions:

$$(2-5) \quad \begin{bmatrix} X_A \\ X_B \end{bmatrix} \equiv \begin{bmatrix} X_{Aa} - X_{A0} \\ X_{Ba} - X_{B0} \end{bmatrix}$$

$$(2-6) \quad \begin{bmatrix} L_1 \\ L_0 \\ L_2 \end{bmatrix} \equiv \begin{bmatrix} L_{1b} - F(X_{A0}, X_{B0}) \\ L_{0b} - X_{A0} \\ L_{2b} - X_{B0} \end{bmatrix}$$

We have the null hypothesis:

$$(2-7) \quad H_0 : \begin{bmatrix} L_1 \\ L_0 \\ L_2 \end{bmatrix} \rightarrow N \left( \begin{bmatrix} A & B \\ I & 0 \\ 0 & I \end{bmatrix} \begin{bmatrix} X_A \\ X_B \end{bmatrix}, \sigma_0^2 \begin{bmatrix} W_1^{-1} & 0 & 0 \\ 0 & W_0^{-1} & 0 \\ 0 & 0 & W_2^{-1} \end{bmatrix} \right)$$

That is, the (observed – computed) vector has a multi-dimensional Normal distribution with expectation given by the first argument, and dispersion given by the second argument in (2-7), where:

$W_0$  ... Weight matrix of the group-0 observations  
 $W_1$  ... Weight matrix of the group-1 observations  
 $W_2$  ... Weight matrix of the group-2 observations  
 $\sigma_0$  ... A priori reference standard deviation (usually set to 1).

Estimate  $X_A$  and  $X_B$  using the Least Squares criterion:

$$(2-8) \quad V_0^T W_0 V_0 + V_1^T W_1 V_1 + V_2^T W_2 V_2 \rightarrow \text{minimum}$$

where:

$\begin{bmatrix} V_0 \\ V_1 \\ V_2 \end{bmatrix}$  ... Post-estimation residual vector.

This leads to the normal equation system for the parameter estimates  $\hat{X}_A$  and  $\hat{X}_B$ :

$$(2-9) \quad \begin{bmatrix} A^T W_1 A + W_0 & A^T W_1 B \\ B^T W_1 A & B^T W_1 B + W_2 \end{bmatrix} \begin{bmatrix} \hat{X}_A \\ \hat{X}_B \end{bmatrix} = \begin{bmatrix} A^T W_1 L_1 + W_0 L_0 \\ B^T W_1 L_1 + W_2 L_2 \end{bmatrix}.$$

Introduce a shorthand notation for the individual elements by writing the normal equation system as:

$$(2-10) \quad \begin{bmatrix} N_{AA} & N_{AB} \\ N_{AB}^T & N_{BB} \end{bmatrix} \begin{bmatrix} \hat{X}_A \\ \hat{X}_B \end{bmatrix} = \begin{bmatrix} U_A \\ U_B \end{bmatrix}.$$

Eliminating the group-A parameters from the second equation in the system:

$$(2-11) \quad \begin{bmatrix} N_{AA} & N_{AB} \\ 0 & \tilde{N}_{BB} \end{bmatrix} \begin{bmatrix} \hat{X}_A \\ \hat{X}_B \end{bmatrix} = \begin{bmatrix} U_A \\ \tilde{U}_B \end{bmatrix}$$

where we have the reduced normal sub-matrices:

$$(2-12) \quad \tilde{N}_{BB} = N_{BB} - N_{AB}^T N_{AA}^{-1} N_{AB}$$

$$(2-13) \quad \tilde{U}_B = U_B - N_{AB}^T N_{AA}^{-1} U_A.$$

Back-substitution in (2-11) gives the parameter estimates:

$$(2-14) \quad \hat{X}_B = \tilde{N}_{BB}^{-1} \tilde{U}_B$$

$$(2-15) \quad \hat{X}_A = N_{AA}^{-1} U_A - N_{AA}^{-1} N_{AB} \hat{X}_B.$$

The cofactor matrices of the group-A and group-B parameters, which when multiplied by the reference standard deviation  $\sigma_0$  give the error covariance matrices of these parameters, are derived by error propagation through (2-14) and (2-15). The cofactor matrices are also known to be the elements of the inverse of the coefficient matrix in (2-10). The resulting group-A and group-B cofactor matrices are:

$$(2-16) \quad Q_{\hat{X}_B \hat{X}_B} = \tilde{N}_{BB}^{-1}$$

$$(2-17) \quad Q_{\hat{X}_A \hat{X}_A} = N_{AA}^{-1} + N_{AA}^{-1} N_{AB} Q_{\hat{X}_B \hat{X}_B} N_{AB}^T N_{AA}^{-1}$$

$$(2-18) \quad Q_{\hat{X}_A \hat{X}_B} = -N_{AA}^{-1} N_{AB} Q_{\hat{X}_B \hat{X}_B}.$$

Equations (2-14) to (2-18) form the desired set of equations for navigation with OTF ASF

calibration. For visualizing the mutual dependence between the group-A and group-B parameters and the relative weighting of the observation groups, it is instructive to write (2-14) and (2-15) in the equivalent form:

$$(2-19) \quad \hat{X}_B = N_{BB}^{-1} B^T W_1 (L_1 - A \hat{X}_A) + N_{BB}^{-1} W_2 L_2$$

$$(2-20) \quad \hat{X}_A = N_{AA}^{-1} A^T W_1 (L_1 - B \hat{X}_B) + N_{AA}^{-1} W_0 L_0$$

and in the equivalent form:

$$(2-21) \quad \hat{X}_B = (B^T D B + W_2)^{-1} B^T D (L_1 - A L_0) + (B^T D B + W_2)^{-1} W_2 L_2$$

$$(2-22) \quad \hat{X}_A = (A^T C A + W_0)^{-1} A^T C (L_1 - B L_2) + (A^T C A + W_0)^{-1} W_0 L_0$$

where:

$$(2-23) \quad D \equiv (W_1^{-1} + A W_0^{-1} A^T)^{-1}$$

$$(2-24) \quad C \equiv (W_1^{-1} + B W_2^{-1} B^T)^{-1}.$$

The above equivalencies are established using the matrix identity:

$$(2-25) \quad (M_{22} - M_{21} M_{11}^{-1} M_{12})^{-1} \equiv M_{22}^{-1} + M_{22}^{-1} M_{21} (M_{11} - M_{12} M_{22}^{-1} M_{21})^{-1} M_{12} M_{22}^{-1}.$$

As an example of the interpretation of the equivalent equations, the form (2-20) shows that the OTF ASF system can be interpreted as using post-adjustment values of ASFs to obtain the position estimates. The form (2-22) shows that the system is equivalent to accounting for the a priori uncertainties in ASFs in the observation weighting.

Two special cases of (2-14) to (2-18) are of interest:

- If there is no external position and time update being used, then  $W_0 = 0$  in (2-9) and the equations still hold.
- If the a priori ASFs are not being adjusted but simply used as constants, then conceptually  $W_2$  is infinite in (2-9) resulting in  $\hat{X}_B = L_2$  being used in (2-15) and  $Q_{\hat{X}_B \hat{X}_B} = W_2^{-1}$  being used in (2-17). The  $\hat{X}_B = L_2$  means  $\hat{X}_{Ba} \equiv X_{B0} + \hat{X}_B = X_{B0} + L_2 \equiv L_{2b}$ , i.e., the a posteriori ASFs are the same as the a priori values, and

$Q_{\hat{x}_B \hat{x}_B} = W_2^{-1}$  means that the a posteriori ASF errors are the same as the a priori ones, as expected in this special case.

### 3. Phase Velocity Error Covariance Model

In [2] Section 4.4 ASF Variations, the scale factor  $w$  is defined as the reciprocal of the phase velocity  $v$ , so that the scale factor error is:

$$(3-1) \quad \Delta w = \Delta \left( \frac{1}{v} \right) = \frac{-\Delta v}{v^2}$$

where  $\Delta v$  is the phase velocity error.

The model in [2] uses as input the scale factor error variance, which we denote by  $C_{\Delta w,0}$ , with default value:

$$(3-2) \quad \sqrt{C_{\Delta w,0}} = 3.6 \times 10^{-4} \text{ microsec/km} \\ = 0.108 \text{ m/km}.$$

It is assumed in [2] that the scale factor error is perfectly correlated between any two points in the operating area. Here, we propose to model the error covariance as a function of the distance between the two points being correlated, in the form:

$$(3-3) \quad C_{\Delta w}(P, Q) = \frac{C_{\Delta w,0}}{\sqrt{3 \left( \frac{d_{PQ}}{\xi} \right)^2 + 1}}$$

where:

- $C_{\Delta w}(P, Q)$  ... Scale factor error covariance between points  $P$  and  $Q$
- $d_{PQ}$  ... Distance between points  $P$  and  $Q$
- $\xi$  ... Scale factor error correlation length
- $C_{\Delta w,0}$  ... Scale factor error variance.

It is assumed that the error covariance is homogeneous (location independent) and isotropic (azimuth independent) throughout the operating area. The two parameters defining the postulated covariance function (3-3) are the variance, which is the value at zero distance, and the correlation length, which is the distance at which the covariance drops to half the variance. Figure 1 plots (3-3) using the default variance (3-2) and sample correlation lengths 750, 500, and 200 km.

The form (3-3) may be referred to as the reciprocal distance covariance form. Other forms may be used to represent the covariance, the only requirement ([3] Section 22) being to use a positive definite function. Positive definiteness of a function is equivalent to non-negativity of the spectrum. The spectrum, or Hankel Transform, of (3-3) is given by:

$$(3-4) \quad \bar{C}_{\Delta w}(\eta) = \frac{C_{\Delta w,0} \xi}{\sqrt{3}} e^{\frac{-\eta \xi}{\sqrt{3}}} \eta.$$

This spectrum is positive for  $\eta > 0$ , so the function  $C_{\Delta w}(d)$  is positive definite. It follows that every covariance matrix derived from (3-3) is also positive definite. Positive definiteness is a requirement for regular covariance matrices. By definition, a square matrix  $M$  is positive definite if ([3], 9-26):

$$(3-5) \quad x M x^T \geq 0$$

for an arbitrary row vector  $x$ , with the equality sign holding only if  $x = 0$ .

### 4. ASF Error Covariance Model

The ASF error covariance model is computed from the scale factor error covariance model (3-3) by covariance propagation through the functional relationship between these two quantities. The functional relationship is an integral of the basic relationship given in [2] Section 4.4. For paths to a Secondary station, the ASF error covariance model accounts for the system area monitor (SAM) control function.

#### 4.1 ASF Error Covariance Between Two User-to-Master paths

The ASF error resulting from scale factor errors along the path from user  $u1$  to Master station  $m1$  is expressed as:

$$(4-1) \quad \Delta ASF_{u1m1} = \int_0^{S_{u1m1}} \Delta w ds_{u1m1}$$

where the integration is along the path, with total length  $S_{u1m1}$  and line element  $ds_{u1m1}$ .

The ASF error covariance between two arbitrary user-to-Master paths,  $u1m1$  and  $u2m2$ , is computed by covariance propagation through (4-1):

$$(4-2) \quad C_{\Delta ASF}(u1m1, u2m2) = \int_0^{S_{u2m2}} \int_0^{S_{u1m1}} C_{\Delta w}(P, Q) ds_{u1m1} ds_{u2m2}$$

where the integrations of the scale factor error covariance function are carried out along the paths  $u1m1$  and  $u2m2$ , with total lengths  $S_{u1m1}$  and  $S_{u2m2}$ , and line elements  $ds_{u1m1}$  and  $ds_{u2m2}$ , respectively.

The ASF error variance of a user-to-Master path is found by evaluating (4-2) for  $u1 = u2$  and  $m1 = m2$ . The ASF error variance computed using (3-3) and (4-2) can be expressed in closed form as a function of path length ([5]):

$$(4-3) \quad C_{\Delta ASF,0}(S) = \frac{2}{3} C_{\Delta w,0} \xi^2 \bullet \left[ \sqrt{3} \frac{S}{\xi} \ln \left( \sqrt{3} \frac{S}{\xi} + \sqrt{3 \left( \frac{S}{\xi} \right)^2 + 1} \right) - \sqrt{3 \left( \frac{S}{\xi} \right)^2 + 1} \right]$$

where  $S$  is the length of the path.

Figure 2 plots the square-root of the result from (4-3), for path lengths from 0 to 3000 km, scale error variance  $C_{\Delta w,0}$  from (3-2), and sample correlation lengths of  $\xi = 200$  km, 500 km, and  $\xi \gg S$ . The case when  $\xi$  is very much larger than the length of the path has the approximation:

$$(4-4) \quad \sqrt{C_{\Delta ASF,0}} \approx \sqrt{C_{\Delta w,0}} S, \quad \xi \gg S.$$

## 4.2 ASF Error Covariance Between Two User-to-Secondary paths

The ASF error along the path from user to Secondary station is defined here to include all ASF-related errors causing Time-of-arrival (TOA) modeling error along the path. This ASF error has two components:

- ASF error resulting from scale factor errors along the user-to-Secondary path
- ASF error resulting from scale factor errors along the SAM-to-Secondary and SAM-to-Master paths. These scale factor errors affect the modeling of the emission delay (ED) and consequently the TOA modeling along the user-to-Secondary path.

The ASF error along the path from user  $u1$  to Secondary  $s1$ , given that the SAM is  $sam1$  and the Master is  $m1$ , is expressed as:

$$(4-5) \quad \Delta ASF_{u1s1} = \int_0^{S_{u1s1}} \Delta w ds_{u1s1} - \int_0^{S_{sam1s1}} \Delta w ds_{sam1s1} + \int_0^{S_{sam1m1}} \Delta w ds_{sam1m1}$$

where the integrations are along the indicated paths.

The ASF error covariance between two arbitrary user-to-Secondary paths,  $u1s1$  and  $u2s2$ , is computed by covariance propagation through (4-5):

$$(4-6) \quad C_{\Delta ASF}(u1s1, u2s2) = \int_0^{S_{u2s2}} \int_0^{S_{u1s1}} C_{\Delta w} ds_{u1s1} ds_{u2s2} - \int_0^{S_{sam2s2}} \int_0^{S_{u1s1}} C_{\Delta w} ds_{u1s1} ds_{sam2s2} + \int_0^{S_{sam2m2}} \int_0^{S_{u1s1}} C_{\Delta w} ds_{u1s1} ds_{sam2m2} - \int_0^{S_{u2s2}} \int_0^{S_{sam1s1}} C_{\Delta w} ds_{sam1s1} ds_{u2s2} + \int_0^{S_{sam2s2}} \int_0^{S_{sam1s1}} C_{\Delta w} ds_{sam1s1} ds_{sam2s2} - \int_0^{S_{sam2m2}} \int_0^{S_{sam1s1}} C_{\Delta w} ds_{sam1s1} ds_{sam2m2} + \int_0^{S_{u2s2}} \int_0^{S_{sam1m1}} C_{\Delta w} ds_{sam1m1} ds_{u2s2} - \int_0^{S_{sam2s2}} \int_0^{S_{sam1m1}} C_{\Delta w} ds_{sam1m1} ds_{sam2s2} + \int_0^{S_{sam2m2}} \int_0^{S_{sam1m1}} C_{\Delta w} ds_{sam1m1} ds_{sam2m2}$$

where the SAM  $sam2$  is controlling the secondary  $s2$  with respect to the master  $m2$ .

## 4.3 ASF Error Covariance Between a User-to-Master and a User-to-Secondary Path

The ASF error covariance between a user-to-Master path,  $u1m1$ , and a user-to-Secondary path,  $u2s2$ , is computed by covariance propagation through the functional relationships of types (4-1) and (4-5):

$$(4-7) \quad C_{\Delta ASF}(u1m1, u2s2) = \int_0^{S_{u2s2}} \int_0^{S_{u1m1}} C_{\Delta w} ds_{u1m1} ds_{u2s2} -$$

$$\int_0^{S_{sam2s2}} \int_0^{S_{u1m1}} C_{\Delta w} ds_{u1m1} ds_{sam2s2} +$$

$$\int_0^{S_{sam2m2}} \int_0^{S_{u1m1}} C_{\Delta w} ds_{u1m1} ds_{sam2m2} .$$

#### 4.4 Differential ASF (DASF) Error Covariance Model

In hybrid operations, in which external position updates are used to control ASF-caused positioning bias, it is of interest to compute the statistical difference in ASF error between the current epoch of a moving receiver and the epoch of the last position update. The size of this differential ASF (DASF) error dictates the position error growth between external updates. It is seen from (4-1) and (4-5) that the DASF error between the paths from two receivers  $u1$  and  $u2$  to a single transmitter  $t1$  is independent of whether  $t1$  is a Master or a Secondary, since the terms in (4-5) involving the SAM cancel out in the difference. The DASF error for the triplet ( $u1$ ,  $u2$ ,  $t1$ ) is expressed as:

$$(4-8) \quad \Delta DASF_{u1u2t1} \equiv \Delta ASF_{u2t1} - \Delta ASF_{u1t1}$$

$$= \int_0^{S_{u2t1}} \Delta w ds_{u2t1} - \int_0^{S_{u1t1}} \Delta w ds_{u1t1} .$$

The DASF error covariance between two arbitrary triplets ( $u1$ ,  $u2$ ,  $t1$ ) and ( $u1$ ,  $u2$ ,  $t2$ ) is computed by covariance propagation through (4-8):

$$(4-9) \quad C_{\Delta DASF}(u1u2t1, u1u2t2) =$$

$$\int_0^{S_{u2t2}} \int_0^{S_{u2t1}} C_{\Delta w} ds_{u2t1} ds_{u2t2} -$$

$$\int_0^{S_{u1t2}} \int_0^{S_{u2t1}} C_{\Delta w} ds_{u2t1} ds_{u1t2} -$$

$$\int_0^{S_{u2t2}} \int_0^{S_{u1t1}} C_{\Delta w} ds_{u1t1} ds_{u2t2} +$$

$$\int_0^{S_{u1t2}} \int_0^{S_{u1t1}} C_{\Delta w} ds_{u1t1} ds_{u1t2} .$$

#### 5. Predicted ASF (PASF) Computation and Error Covariance Model

Error analysis using (4-9) is based on the conventional differential positioning concept, which relies on the assumption that the ASF errors at the current receiver location are approximately equal to those at the location of the last position update. It is proposed here to improve the differential concept by predicting the ASF error (instead of simply assuming equality) based on the estimated ASF errors at the last update. As the prediction algorithm, we choose the one based on

the criterion of minimum prediction error variance ([3] Section 9). In this technique, the ASF errors along the paths from receiver  $u2$  to an arbitrary transmitter  $tp$  is predicted from the estimated ASF errors along the paths from reference receiver  $u1$  to transmitters  $t1$ ,  $t2$ , ...,  $tm$ . The technique is termed least squares collocation as explained in [3] Section 11. The following description follows [3] Sections 16 and 17.

The linearized observation model is written as:

$$(5-1) \quad l = AX + t + n$$

where:

- $l$  ... TOA residual vector after linearization around the a priori receiver coordinates and ASFs
- $A$  ... Known geometry matrix, expressing the effects of parameter corrections  $X$  on the residuals  $l$
- $X$  ... Parameter correction vector to be estimated, containing corrections to the a priori East, North, Time coordinates of the receiver
- $AX$  ... "Systematic part" of  $l$
- $t$  ... "Signal part" of  $l$ , consisting of the ASF corrections to be estimated
- $n$  ... "Noise part" of  $l$ , containing the TOA measurement errors.

Along with the estimation of  $X$  and  $t$  we will predict a signal vector  $u$ , containing ASF corrections at an arbitrary user location and related to  $t$  by the signal covariances:

$$(5-2) \quad C_{uu} \equiv \text{cov}(u, u) = M\{uu^T\}$$

$$(5-3) \quad C_{ut} \equiv \text{cov}(u, t) = M\{ut^T\}$$

$$(5-4) \quad C_{tt} \equiv \text{cov}(t, t) = M\{tt^T\}$$

where  $M\{\cdot\}$  is the averaging operator. These ASF error covariances are derived from the fundamental covariance function (3-3) of scale factor error using the formulas in Section 4.

The covariance matrix of TOA measurement errors is denoted:

$$(5-5) \quad C_{nn} = E\{nn^T\}$$

where  $E\{\cdot\}$  is the expectation operator.

It is assumed that the a priori parameter vector  $X_0$ , used to generate the linearized model (5-1), has the following error covariance matrix:

$$(5-6) \quad W_0^{-1} = E\{\delta X_0 \delta X_0^T\}$$

where the prefix  $\delta$  denotes the error in the prefixed quantity.

The signal vectors  $t$  and  $u$  are combined into one signal vector  $s$ :

$$(5-7) \quad s = \begin{bmatrix} t \\ u \end{bmatrix}$$

with the following covariances:

$$(5-8) \quad C_{ss} = \begin{bmatrix} C_{tt} & C_{tu} \\ C_{ut} & C_{tt} \end{bmatrix}; \quad C_{st} = \begin{bmatrix} C_{tt} \\ C_{ut} \end{bmatrix}.$$

The minimization principle for least squares collocation is:

$$(5-9) \quad s^T C_{ss}^{-1} s + n^T C_{nn}^{-1} n + X^T W_0 X \rightarrow \text{minimum}$$

which is generalized from [3] (16-15) by including the a priori parameter weight  $W_0$ .

The resulting parameter estimates, along with their a posteriori error covariances, are given by:

$$(5-10) \quad \hat{X} = G l$$

$$(5-11) \quad \hat{s} = H(l - A\hat{X})$$

$$(5-12) \quad E_{XX} = (A^T \bar{C}^{-1} A + W_0)^{-1}$$

$$(5-13) \quad E_{ss} = C_{ss} - C_{st} \bar{C}^{-1} C_{ts} + H A E_{XX} A^T H^T$$

where:

$$(5-14) \quad G \equiv (A^T \bar{C}^{-1} A + W_0)^{-1} A^T \bar{C}^{-1}$$

$$(5-15) \quad H \equiv C_{st} \bar{C}^{-1}$$

$$(5-16) \quad \bar{C} \equiv C_{tt} + C_{nn}.$$

In the application of this report the signal vector  $t$ , which forms part of  $s$ , contains the ASFs at the location of the position update. The accuracy of position update is reflected in the a priori weight matrix  $W_0$ . The signal vector  $u$ , which forms the remaining part of  $s$ , contains the ASFs at an

arbitrary location for which predicted ASFs are desired.

## 6. Navigation Errors Implied by ASF Calibration and TOA Measurement Errors

The error covariance of estimated (East, North, Time) parameters can be expressed in the nominal form (see (2-17)):

$$(6-1) \quad E_{ENT} = (A^T W_1 A)^{-1} + (A^T W_1 A)^{-1} A^T W_1 E_{ASF} W_1 A (A^T W_1 A)^{-1}$$

where  $W_1$  is the inverse of the TOA measurement error covariance matrix and  $E_{ASF}$  is the ASF error covariance matrix. Here, the  $B$  matrix has been taken as an identity matrix under the assumption that the ASF parameters are ordered in the same way as the TOA observations. The first term of (6-1) accounts for the effects of TOA measurement errors, while the second term accounts for the effects of ASF calibration errors. For the verification runs and tests of this report, various cases of the ASF error covariance matrix  $E_{ASF}$  appearing in (6-1) were considered, as defined in the following sections.

### 6.1 Navigation using a priori ASFs

When using an a priori ASF model with no adjustment of the ASF values, the  $E_{ASF}$  to use in (6-1) is equal to the a priori ASF error covariance matrix as computed using (4-2), (4-6), and (4-7):

$$(6-2) \quad E_{ASF(1)} = C_{\Delta ASF}.$$

### 6.2 Navigation using a posteriori ASFs with no position/time update

When adjusting the a priori ASF values simultaneously with the navigation estimation, but without using any external position and time parameter information, the  $E_{ASF}$  to use in (6-1) is the a posteriori ASF error covariance matrix of the adjustment (see (2-16)):

$$(6-3) \quad E_{ASF(2)} = \left[ W_1 + C_{\Delta ASF}^{-1} - W_1 A (A^T W_1 A)^{-1} A^T W_1 \right]^{-1}.$$

### 6.3 Navigation using a posteriori ASFs with position/time update at the user location

When adjusting the a priori ASF values simultaneously with the navigation estimation, and using external position and time parameter information as represented in the a priori weight matrix  $W_0$ ,  $E_{ASF}$  is the a posteriori ASF error covariance matrix of the adjustment (see (2-16)):

$$(6-4) \quad E_{ASF(3)} = \left[ W_1 + C_{\Delta ASF}^{-1} - W_1 A (A^T W_1 A + W_0)^{-1} A^T W_1 \right]^{-1}.$$

In this case, the error covariance matrix of estimated (East, North, Time) parameters is a modified form of (6-1):

$$(6-5) \quad E_{ENT(3)} = \left( A^T W_1 A + W_0 \right)^{-1} + \left( A^T W_1 A + W_0 \right)^{-1} A^T W_1 E_{ASF(3)} W_1 A \left( A^T W_1 A + W_0 \right)^{-1}.$$

### 6.4 Navigation using predicted ASFs

In this case the ASFs used in the navigation are predicted from ASFs calibrated at a reference user location. The ASFs are calibrated at the reference location using a position/time update at that location. The error analysis for this calibration is given by (6-4) or, equivalently, (5-13) evaluated for  $s = t$ . The  $E_{ASF}$  to use in (6-1) is given by (5-13) evaluated for  $s = u$ :

$$(6-6) \quad E_{ASF(4)} = E_{uu}.$$

In evaluating (6-6), the required matrices  $A$ ,  $C_{tt}$ ,  $C_{mm}$ , and  $W_0$  all refer to the reference location at which the ASFs are calibrated.

### 6.5 Navigation using predicted/a posteriori ASFs

In this case the predicted ASFs are adjusted within the navigation estimation, hence the  $E_{ASF}$  to use in (6-1) is the a posteriori ASF error covariance matrix of the adjustment:

$$(6-7) \quad E_{ASF(5)} = \left[ W_1 + E_{uu}^{-1} - W_1 A (A^T W_1 A)^{-1} A^T W_1 \right]^{-1}.$$

### 6.6 Navigation using differential ASFs

In the conventional differential Loran concept, the  $E_{ASF}$  to use in (6-1) is the differential ASF (DASF) error covariance matrix with respect to the reference station, as computed using (4-9), plus the ASF calibration error covariance, as computed at the reference location using (6-4):

$$(6-8) \quad E_{ASF(6)} = C_{\Delta DASF} + E_{ASF(3)}^{reference}.$$

As noted above (6-6), the second term of (6-8) is equivalent to evaluating (5-13) for  $s = t$  at the reference location of the position and time update.

## 7. OTF ASF Calibration Tests

This section describes the verification and validation tests performed on the on-the-fly ASF calibration equations given in the previous sections. The tests are limited to the covariance analysis approach. The tests used the geometry of five Loran chains in the eastern U.S., the phase velocity error covariance model described in Section 3, and a postulated TOA measurement error model. Notes on the implementation of the tests are given, followed by a discussion of the numerical results.

### 7.1 Implementation Notes

#### Map Projection

The tests used planar computations. The planar East and North components of a given path is computed from spherical coordinates as follows:

$$(7-1) \quad \Delta E_{ij} = (\lambda_j - \lambda_i) R_e \cos \varphi_0$$

$$(7-2) \quad \Delta N_{ij} = (\varphi_j - \varphi_i) R_e$$

where:

$\varphi_i, \lambda_i$  ... Latitude, Longitude of endpoint  $i$

$\varphi_j, \lambda_j$  ... Latitude, Longitude of endpoint  $j$

$\varphi_0$  ... Reference latitude (mid-latitude in the area)

$R_e$  ... Average radius of the earth.

#### Double Line Integration

The implementation of the basic double line integral of the covariance function (3-3) involves the combined use of a closed form expression for the inner integral, followed by Romberg numerical

integration of the outer integral. The resulting computational speed has been found satisfactory. Future studies should investigate the use of covariance functions in spherical coordinates ([2] Section 23) and develop corresponding closed form and/or numerical implementation for the double line integral.

The basic double line integral of the covariance function (3-3) along the paths point1-to-point2 and point3-to-point4 can be written in the form:

$$(7-3) \quad I = \int_0^{s_{12}} \int_0^{s_{34}} \frac{C_{\Delta w,0} ds_{34} ds_{12}}{\sqrt{\frac{3}{\xi^2} (s_{12}^2 + s_{34}^2 + a_0 + a_1 s_{12} + a_2 s_{34} + a_3 s_{12} s_{34}) + 1}}$$

where:

- $S_{12}$  ... Length of path from point 1 to point 2
- $S_{34}$  ... Length of path from point 3 to point 4
- $s_{12}$  ... Coordinate of integration point along path 1-to-2, reckoned from 1
- $s_{34}$  ... Coordinate of integration point along path 3-to-4, reckoned from 3

and:

$$(7-4) \quad S_{12} = \sqrt{\Delta E_{12}^2 + \Delta N_{12}^2}$$

$$(7-5) \quad S_{34} = \sqrt{\Delta E_{34}^2 + \Delta N_{34}^2}$$

$$(7-6) \quad a_0 = \Delta E_{13}^2 + \Delta N_{13}^2$$

$$(7-7) \quad a_1 = -2 \frac{\Delta E_{13} \Delta E_{12} + \Delta N_{13} \Delta N_{12}}{S_{12}}$$

$$(7-8) \quad a_2 = 2 \frac{\Delta E_{13} \Delta E_{34} + \Delta N_{13} \Delta N_{34}}{S_{34}}$$

$$(7-9) \quad a_3 = -2 \frac{\Delta E_{12} \Delta E_{34} + \Delta N_{12} \Delta N_{34}}{S_{12} S_{34}}$$

Solving the inner integral of (7-3) in closed form results in ([5]):

$$(7-10) \quad I = \int_0^{s_{12}} \left[ \sinh^{-1} \left( \frac{2S_{34} + a_2 + a_3 s_{12}}{D} \right) - \sinh^{-1} \left( \frac{a_2 + a_3 s_{12}}{D} \right) \right] ds_{12}$$

where:

$$(7-11) \quad D = \sqrt{\left( \frac{4\xi^2}{3} + 4a_0 - a_2^2 \right) + 2(2a_1 - a_2 a_3) s_{12} + (4 - a_3^2) s_{12}^2}$$

In the implementation, the integral (7-10) is computed using the Romberg numerical integration technique ([4] Section 4.3). The inverse hyperbolic sine is calculated using the equality:

$$(7-12) \quad \sinh^{-1}(x) \equiv \ln \left( x + \sqrt{x^2 + 1} \right).$$

For verification purposes, the integral (7-3) was computed by double numerical Romberg integration and the results compared with the use of (7-10) and with the special case (4-3). The results from numerical integration agreed with those from the closed form expressions to within round-off error. For the test runs of this report, the use of the combined numerical/analytical integration with (7-10) produced a speed-up factor of 15 compared to the use of purely numerical double integration with (7-3).

### Covariance Analysis Inputs

The  $i^{\text{th}}$  row of the design matrix  $A$  corresponds to the  $i^{\text{th}}$  transmitter being observed and contains the sine and cosine of the bearing angle from the receiver to the transmitter:

$$(7-13) \quad A_i = [b \sin_i \quad b \cos_i \quad 1].$$

The TOA measurement error covariance matrix is assumed diagonal. The  $i^{\text{th}}$  diagonal element is the following assumed measurement error variance (meters<sup>2</sup>):

$$(7-14) \quad \sigma_{obs,i}^2 = 50^2 + \left( 10 + 3.66 \times 10^{-5} d_{km}^2 \right)^2$$

where  $d_{km}$  is the distance in kilometers between the receiver and the  $i^{\text{th}}$  transmitter. The first term in (7-14) accounts for clock and other errors while the second term is a rough fit to the SNR values of a test data set in the Madison, Wisconsin area.

The a priori ASF error covariance matrices are computed using (4-2), (4-6), and (4-7). The a priori parameter weight matrix  $W_0$  is assumed diagonal and is computed from input standard errors of the East, North, and Time updates.

## 7.2 Numerical Results

Figure 3 plots the geometry of SAM control of the various Loran transmitters of the five chains used in the tests. Secondary IDs are written close to the applicable Secondary-to-SAM path to aid the reading of the figure. For example, transmitter 8

(Gillette) is controlled by the Bismarck SAM relative to Master 6 (Havre). The paths to the SAMs enter the ASF error covariance models of Section 4.

Figure 4 plots the location of the eleven test users (U0, U1, ..., U10), along with the transmitters of the five Loran chains, used in this report. User 0 (U0) is in Madison, WI. Users U1, U2, U3 are 500, 1000, and 1500 km due west of U0, respectively. Users U4, U5, U6 are 500, 1000, 1500 km due south of U0, respectively. Users U7, U8, U9, U10 are positioned in the periphery of the coverage area.

Table 1 gives the nominal error parameters used in the tests. Exceptions to the nominal values will be explicitly noted in the discussion. The nominal scale factor error has a nominal standard deviation of 0.108 m/km and a correlation length of 200 km. The nominal (East, North, Time) parameter update has a standard error of (20, 20, 20) meters. The TOA measurement errors are modeled by (7-14).

Table 2 shows the test result verifying successfully the implementation of the Romberg numerical integration using (7-10) against the closed expression (4-3). The table also gives an idea of the effects of SAM control on the ASF error model, by comparing the last two columns of the table.

Figure 5 plots three levels of error ellipse refinement at each test user location. In the order of decreasing ellipse size, the three levels correspond to navigation using:

- Case 1: a priori ASFs, (6-1) and (6-2)
- Case 2: a posteriori ASFs with no position/time update, (6-1) and (6-3)
- Case 3: predicted/a posteriori ASFs with position/time update at the U0 location, (6-1) and (6-7).

The minimum and maximum 2DRSS position error over all test users for these navigation cases are given in Table 3. The 2DRSS is defined as twice the square-root of the sum of the squares of the east and north standard errors.

The Case 1 2DRSS error ranges from 126 m (U5) in the central area to 298 m (U9) in Maine. The Case 2 2DRSS error ranges from 88 m (U5) to 206 m (U9). The Case 3 2DRSS error ranges from 72 m (U5) to 184 m (U9). In going from Case 1 to Case 2, the 2DRSS error is reduced by 27%, from a mean of 177 m down to 129 m. In going from

Case 2 to Case 3, the 2DRSS error is reduced by about 40% close to the reference calibration location, with diminishing effect away from the reference. The reduction is about (25%, 20%, 10%) for users (500 km, 1000 km, 1500 km) away from the calibration reference.

Figure 6 is a variation of Figure 5 (nominal case) to see the effect of increasing the scale factor error correlation length from 200 to 500 km. The corresponding minimum and maximum 2DRSS position errors are given in Table 3 as Cases 1a, 2a, and 3a. In going from Case 1 to 1a, the 2DRSS error increases by 20-30% for the different users. In going from Case 2 to 2a, the 2DRSS error increases or decreases by 1-7%. In going from Case 3 to 3a, the 2DRSS error decreases by 1-7%. In short, comparison of Figures 5 and 6 shows 20-30% larger outer ellipses due to the increased error correlation length, with the effects on the two inner ellipses being less than 10%.

Figure 7 is a variation of Figure 5 to see the effect of doubling the scale factor standard error, from 0.108 m/km to 0.216 m/km. Note the factor-of-two change in the plotting scale for the error ellipses between Figures 5 and 7. As expected, the outer ellipses (navigation with a priori ASFs) are increased by close to 100%. In fact, examination of (6-1) and (6-2) shows that the ASF-only contribution to the error ellipse is increased by exactly 100%. The size of the second-to-largest error ellipse at each site (navigation with a posteriori ASFs with no position/time update) is increased by 65-75%. The size of the smallest error ellipse at each site (navigation using predicted/a posteriori ASFs) is increased by 10-65%, with the users farthest away from the reference calibration location (U0) receiving the largest percentage increase. Table 3 gives the minimum and maximum 2DRSS errors corresponding to Figure 7 as Cases 1b, 2b, and 3b.

Table 3 gives, in addition to the results referred to above, the results for navigation using:

- Case 4: a posteriori ASFs with position/time update at the user location, (6-4) and (6-5)
- Case 5: differential ASFs relative to U0, (6-1) and (6-8).

For completeness, Table 3 also gives the resulting standard error of the time parameter for all test cases, in addition to the minimum and maximum 2DRSS errors.

The Case 4 2DRSS error is close to 50 meters for all test users, indicating the direct influence of the position and time updates. The Case 5 results are poor, illustrating that the conventional differential concept of relying on the equality of ASF errors between the user and the reference location works only for very short distances from the reference.

In another test of navigation using predicted/a posteriori ASFs, the standard error of time update at User 0 was increased from 20 to 500 m to see the importance of the time update. The resulting ASF error at each site increased by 5-30%, with the largest increase occurring close to User 0. However, the corresponding 2DRSS position error increase was only 1-6%.

## 8. Summary and Recommendations

This paper presents a covariance analysis of multichain navigation with on-the-fly ASF calibration, an a priori ASF/ED error model, and an ASF/ED prediction technique. As a general recommendation, the algorithms developed in this paper should be implemented in an end-to-end system as described in [1]. The system should be tested and tuned with real data, all-in-view receiver, and truth navigation using GPS. The following specific recommendations are made.

The covariance function (3-3) of ASF/ED errors should be fitted to real data in various geographic regions within the operating area. Sensitivity of the prediction and error analysis results to the possible range of covariance parameter values should be examined to determine whether it is necessary to use regionally valid sets of covariance parameters.

In stand-alone Loran, where no position or time update is available from an external source, a posteriori ASFs should be used, i.e., adjust the a priori ASF model, using its full error covariance matrix, along with the navigation estimation of user position and time parameters. A 27% improvement over the use of a priori ASFs was achieved in the nominal tests. The specific improvement depends on the TOA measurement errors and observing geometry.

In hybrid operations, in which an external position/time update is available (e.g., from GPS or surveyed airport position), the position/time update should be used to calibrate the ASFs using least squares. Least squares collocation should be used to predict the ASF errors at the user location

based on calibrated ASF errors at the nearest reference location. The full error covariance of predicted ASFs should be used in the navigation estimation.

The described collocation equations predict the ASF errors along user-to-transmitter paths based on calibrated ASF errors along arbitrary paths, given an underlying covariance function of scale factor error. It is recommended that this prediction technique be considered as a tool in a possibility to broadcast ASF corrections along predetermined paths from which Loran users can predict ASF corrections along their specific user-to-transmitter paths.

## REFERENCES

- [1] "Loran-C Augmentation for GPS and GPS/WAAS, Volume 1: All-In-View Algorithm Development", Illgen Simulation Technologies, Inc., IST2000-R-242, October 2000.
- [2] "Loran-C Availability Models", The Analytical Sciences Corporation, TIM-07462-1, December 1994.
- [3] Advanced Physical Geodesy, H. Moritz, ISBN 0-85626-195-5, Abacus Press, England, 1980.
- [4] Numerical Recipes, Press et al, ISBN 0-521-43064-X, Cambridge University Press, 1986-1992.
- [5] R. Stoeckly, ISTI, private communication, July 2000.

## BIOGRAPHY

Jaime Y. Cruz is a Principal Engineer with the Navigation and Communications Division at ISTI. He has worked for five years on navigation with the Global Positioning System and the FAA's Wide Area Augmentation System. His previous experience included local and global gravity field modeling for ICBM targeting, positioning of ground targets using a satellite-borne laser ranging system, satellite orbit estimation, and development of an airborne gravity measuring system for oil exploration. Dr. Cruz received his MS (1982) and Ph.D. (1985) in geodesy from The Ohio State University.

## ACKNOWLEDGEMENT

The work described in this paper was sponsored by the "FAA AND-740 Loran-C Augmentation for GPS and GPS/WAAS" Program under Grant 99-G-038.

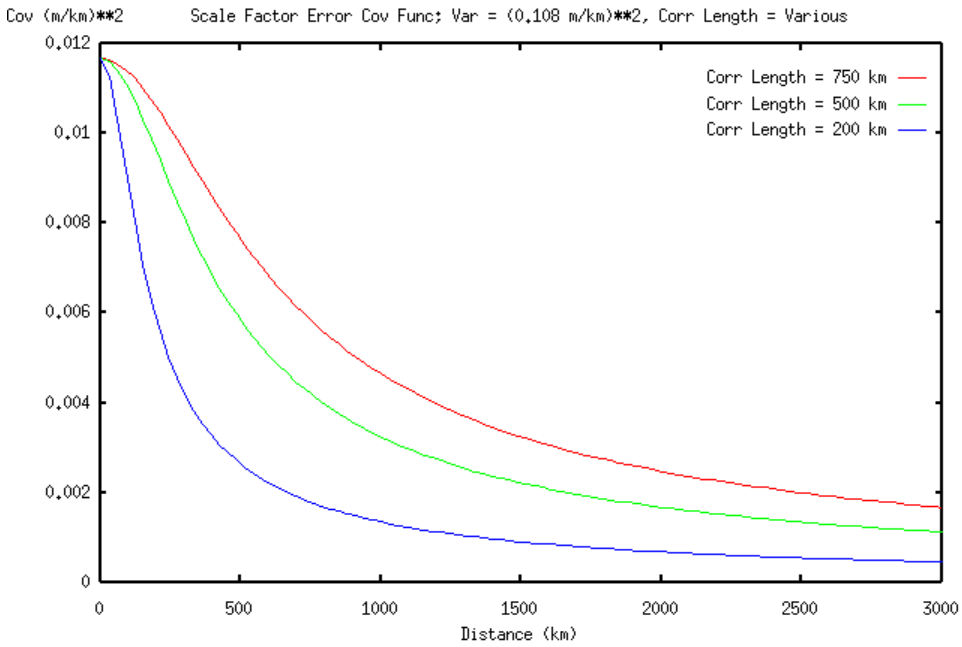


**Figure 1. Scale factor error covariance function.**  
**Variance = (0.108 m/km)\*\*2 and sample correlation lengths = 750, 500, and 200 km.**

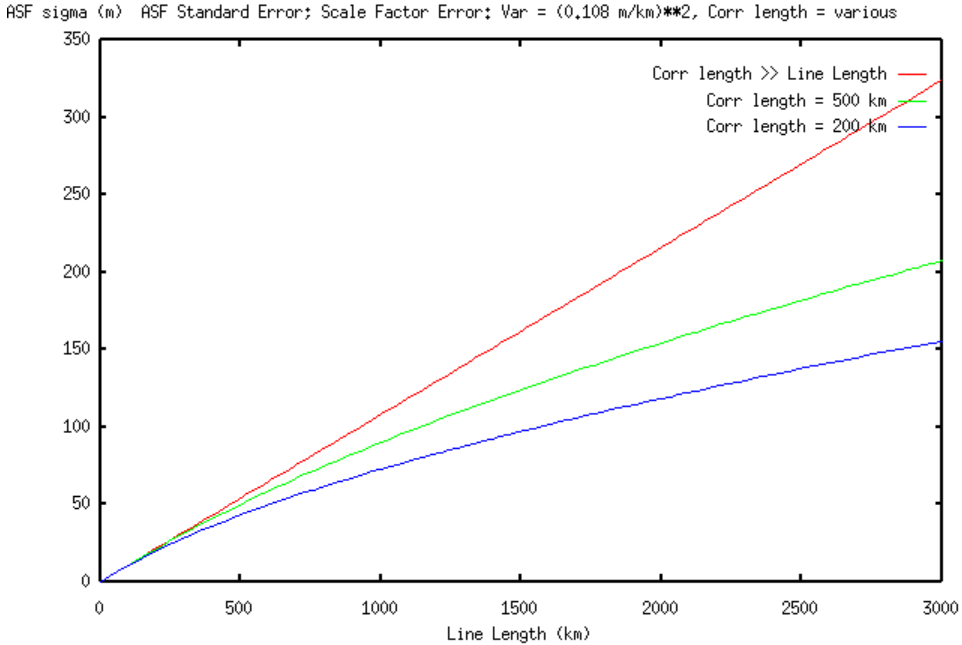


**Figure 2. ASF standard error as a function of path length.**  
**Based on double integral of scale factor error covariance function with variance (0.108 m/km)\*\*2 and various correlation lengths.**

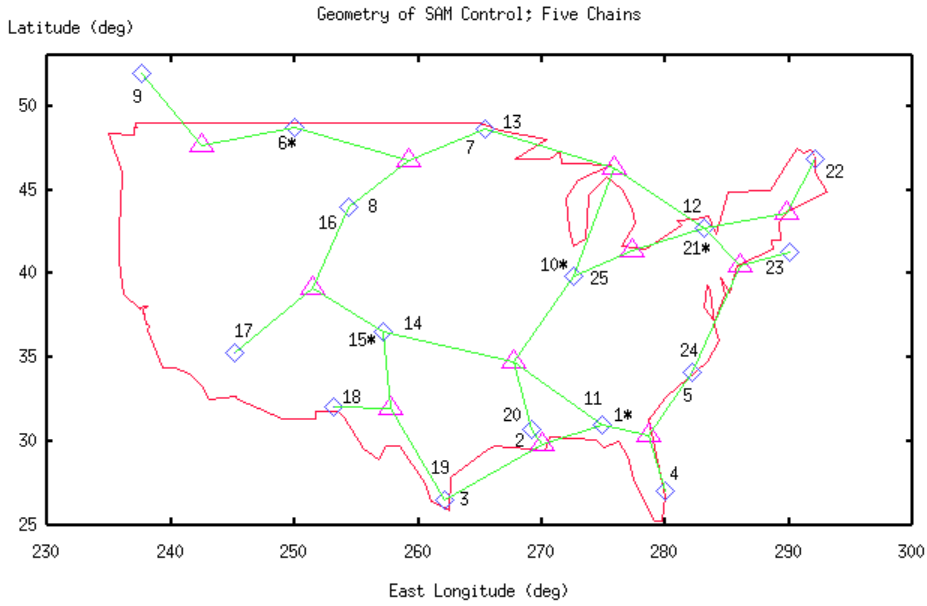


**Figure 3. Geometry of SAM control for Loran transmitters.**  
**Triangle: SAM; Diamond: Transmitter; ID with Asterisk: Master.**  
**Secondary IDs are written close to the applicable Secondary-to-SAM path.**

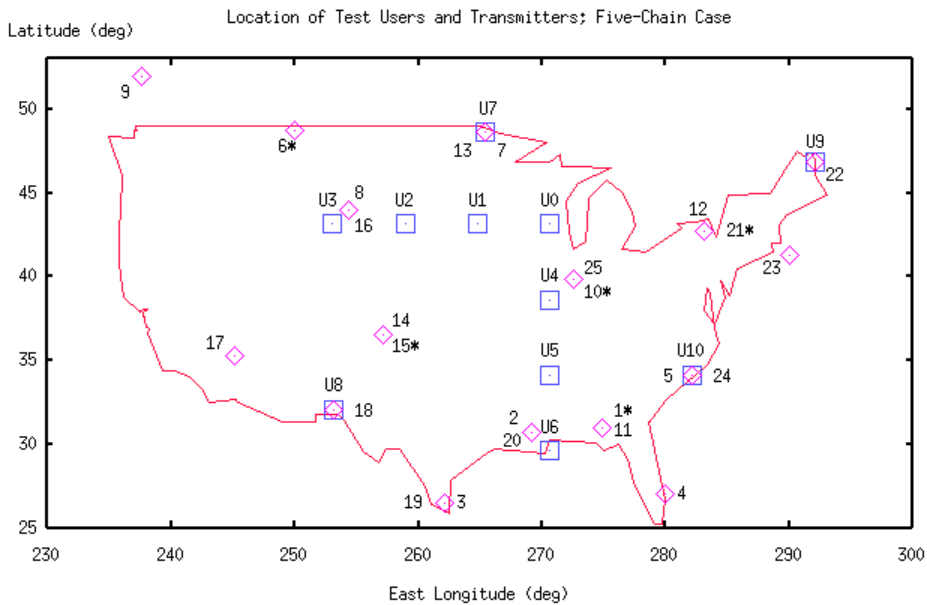


**Figure 4. Location of test users and transmitters.**  
**Diamond: Transmitter; Square: User; ID with Asterisk: Master.**  
**User U0 is in Madison, WI.**

**Table 1. Nominal error covariance parameters used in the tests.  
 Exceptions for certain tests will be explicitly stated.  
 The scale factor error covariance function is given by Equation (3-3).**

**Scale Factor Error Covariance Parameters:**

std (m/km)	cnot (m**2/km**2)	corrl (km)
0.108	0.011664	200.0

**Uncorrelated Std Error of A Priori E, N, T update:**

20.0 m	20.0 m	20.0 m
--------	--------	--------

**Uncorrelated TOA measurement error variance (m\*\*2):**

$$\sigma_{obs}^2 = 50^2 + (10 + 3.66 \times 10^{-5} d_{km}^2)^2$$

**Table 2. Standard deviation of ASF error along User0-to-transmitter paths, resulting from double line integration of the scale factor error covariance function along each path. No emission delay (ED) effects means the integrals along Secondary-to-SAM paths have been excluded. Computation is based on Equations (4-2) and (4-6) applied to the same transmitter.**

**Table Legend:**

**Dist ... User0 distance to transmitter**

**(1) ... User0 Std ASF Err; No ED effects; From closed form integral, Equation (4-3)**

**(2) ... User0 Std ASF Err; No ED effects; Romberg integration based on Equation (7-10)**

**(3) ... User0 Std ASF Err; w/ ED effects; Romberg integration based on Equation (7-10)**

GRI	Sta	Name	Seq No.	Dist (km)	(1) (m)	(2) (m)	(3) (m)
7980	M	Malone	1	1394.822	92.27	92.26	92.26
7980	W	Grangeville	2	1384.565	91.79	91.79	105.44
7980	X	Raymondville	3	1981.928	117.67	117.67	112.97
7980	Y	Jupiter	4	1957.050	116.66	116.66	118.62
7980	Z	CarolinaBeach	5	1400.817	92.54	92.54	91.28
8290	M	Havre	6	1866.237	112.93	112.93	112.93
8290	W	Baudette	7	755.041	59.11	59.11	79.97
8290	X	Gillette	8	1390.732	92.07	92.07	103.82
8290	Y	WilliamsLake	9	2980.359	154.73	154.74	170.56
8970	M	Dana	10	396.583	35.76	35.76	35.76
8970	W	Malone	11	1394.822	92.27	92.26	113.61
8970	X	Seneca	12	1066.648	76.22	76.22	100.37
8970	Y	Baudette	13	755.041	59.11	59.11	74.69
8970	Z	BoiseCity	14	1369.849	91.10	91.10	100.88
9610	M	BoiseCity	15	1369.849	91.10	91.10	91.10
9610	V	Gillette	16	1390.732	92.07	92.07	98.74
9610	W	Searchlight	17	2336.461	131.54	131.54	140.31
9610	X	LasCruces	18	1934.063	115.72	115.73	131.25
9610	Y	Raymondville	19	1981.928	117.67	117.67	118.69
9610	Z	Grangeville	20	1384.565	91.79	91.79	113.42
9960	M	Seneca	21	1066.648	76.22	76.22	76.22
9960	W	Caribou	22	1869.089	113.04	113.05	127.55
9960	X	Nantucket	23	1662.111	104.27	104.27	111.90
9960	Y	CarolinaBeach	24	1400.817	92.54	92.54	89.81
9960	Z	Dana	25	396.583	35.76	35.76	49.76

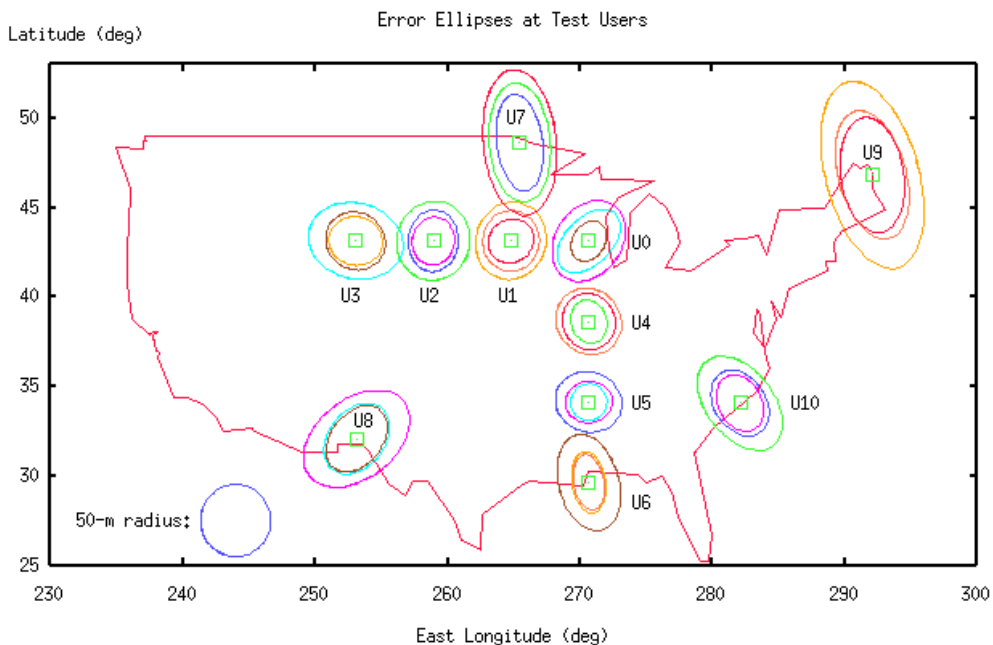


**Figure 5. Three levels of error ellipse refinement at each test user location, corresponding to navigation using: (a) a priori ASFs, (b) a posteriori ASF with no position/time update, and (c) a posteriori ASF with position/time update at the User 0 (U0) location.**

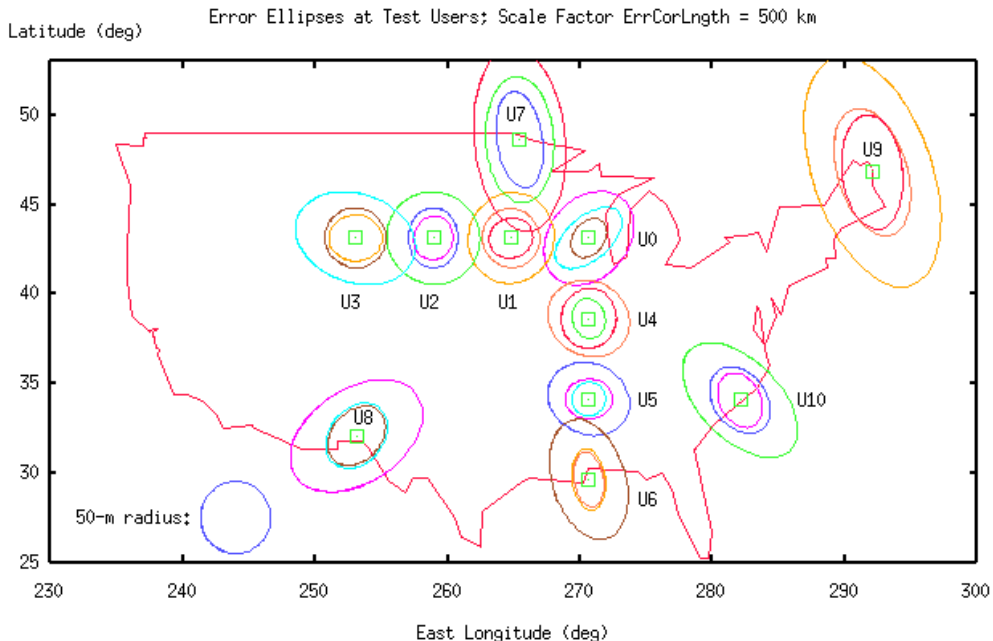


**Figure 6. Same as Figure 5, except that scale factor error correlation length = 500 km.**

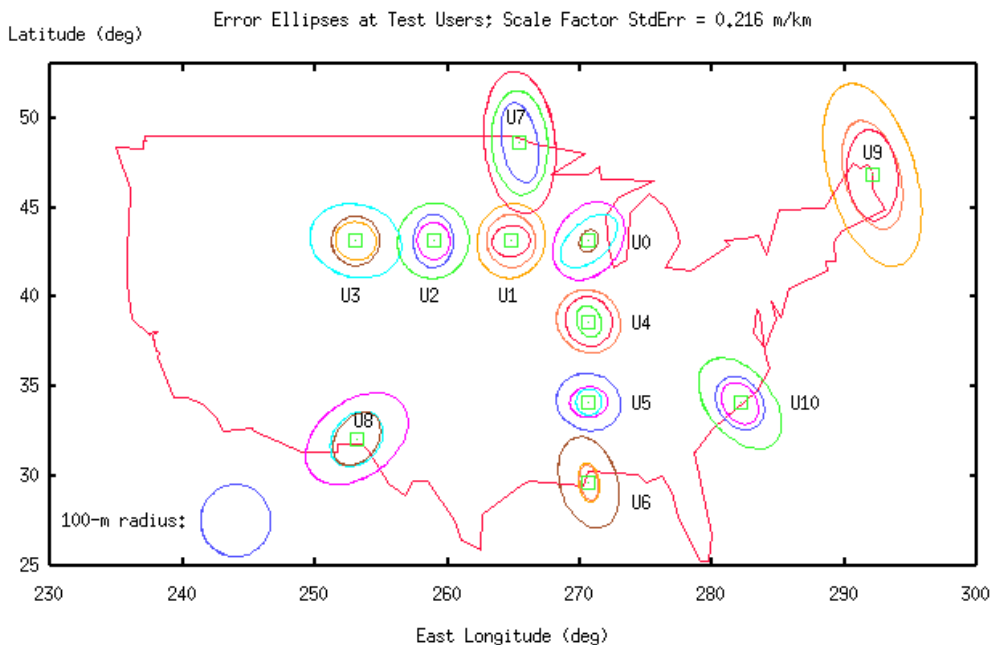


Figure 7. Same as Figure 5, except that the scale factor standard error is doubled to 0.216 m/km.

**Table 3. Minimum and maximum 2DRSS position error and time parameter standard error. Associated test user ID is given in parentheses. Units: meters. Cases 1a, 2a, 3a have scale factor error correlation length = 500 km. Cases 1b, 2b, 3b have scale factor standard error = 0.216 m/km.**

Navigation Case	2DRSS		Time Sigma	
	Min	Max	Min	Max
1. A priori ASFs	126 (U5)	298 (U9)	44 (U10)	80 (U9)
2. A posteriori ASFs with no pos/time update	88 (U5)	206 (U9)	32 (U10)	61 (U9)
3. Predicted/a posteriori ASFs (ASFs are predicted from User 0 calibrated ASFs, with pos/time update at the User 0 location only)	72 (U5)	184 (U9)	23 (U10)	45 (U8)
4. A posteriori ASFs with pos/time update at the user location	47 (U5)	53 (U9)	16 (U10)	18 (U1)
5. Differential ASFs relative to U0 (min/max excludes U0)	115 (U4)	333 (U9)	30 (U1)	102 (U8)
1a. A priori ASFs	155 (U5)	374 (U9)	60 (U10)	108 (U9)
2a. A posteriori ASFs with no pos/time update	87 (U5)	207 (U9)	33 (U10)	63 (U9)
3a. Predicted/a posteriori ASFs (ASFs are predicted from User 0 calibrated ASFs, with pos/time update at the User 0 location only)	66 (U5)	181 (U9)	22 (U4)	44 (U8)
1b. A priori ASFs	243 (U5)	579 (U9)	85 (U10)	154 (U9)
2b. A posteriori ASFs with no pos/time update	125 (U6)	347 (U9)	52 (U10)	104 (U9)
3b. Predicted/a posteriori ASFs (ASFs are predicted from User 0 calibrated ASFs, with pos/time update at the User 0 location only)	83 (U0)	290 (U9)	26 (U0)	70 (U8)



**Jaime Cruz**